How a Broken Egg Attractor Has Influenced the Dynamics of My Life

AUTHOR(S):

Ueda, Yoshisuke

CITATION:

Ueda, Yoshisuke. How a Broken Egg Attractor Has Influenced the Dynamics of My Life. Procedia IUTAM 2012, 5: 7-26

ISSUE DATE:

2012

URL:

http://hdl.handle.net/2433/161162

IUTAM Symposium on 50 Years of Chaos: Applied and Theoretical

How a Broken Egg Attractor Has Influenced the Dynamics of My Life[1]

Yoshisuke Ueda[a]*

[a] *Waseda University and Emeritus Professor of Kyoto University*

Abstract

First, the Broken Egg Phenomenon (BEgg) which constitutes this symposium's starting point is presented. It was observed accidentally in the course of the author's analog computer experiments for a Periodically Forced Self-Oscillatory System, just 50 years and 5 days ago. Then, experimental researches are given from another study conducted in accordance with the BEgg phenomenon which was implemented as an electronic circuit. Finally, the prescriptive systems are proposed in order to survey the phenomena which occur in Periodically Forced Self-Oscillatory Systems. Among various steady states in the systems, regular (predictable) phenomena and their bifurcation sets are presented, covering all such phenomena that are readily observed, perhaps excepting some phenomena of so-called second kind. Various chaotic attractors are also collected, and it is shown that global bifurcations and classification of chaotic attractors are often related, but it seems to be extremely difficult to describe them completely.

Keywords: Broken Egg Attractor; Phenomenon of Synchronization; Analog Computer Simulation; Frequency Entrainment; Quenching; Asynchronous Beat Oscillation; Quasi- or Almost-Periodic Oscillation; Chaotic Oscillation; Phase Portrait; Bifurcation Set

1. Gratitude for all

Please Refer to the Author's Address in the Transactions.

2. Origin of My Researches in Nonlinear Dynamics

(a) Meeting with Broken Egg Phenomenon

This item is an obligatory introduction of the Broken Egg Phenomenon which was observed accidentally in the course of the author's analog computer experiments for a Periodically Forced Self-Oscillatory System, just 50 years and 5 days ago. Figure 1 shows output of an analog simulation of the Eq.1.

[1] IUTAM Symposium on 50 Years of Chaos: Applied and Theoretical, Nov. 28-Dec. 2, 2011, Kyoto University, Clock Tower Centennial Hall, Kyoto, JAPAN

Email address: ueda.yoshi@gmail.com (Yoshisuke Ueda)

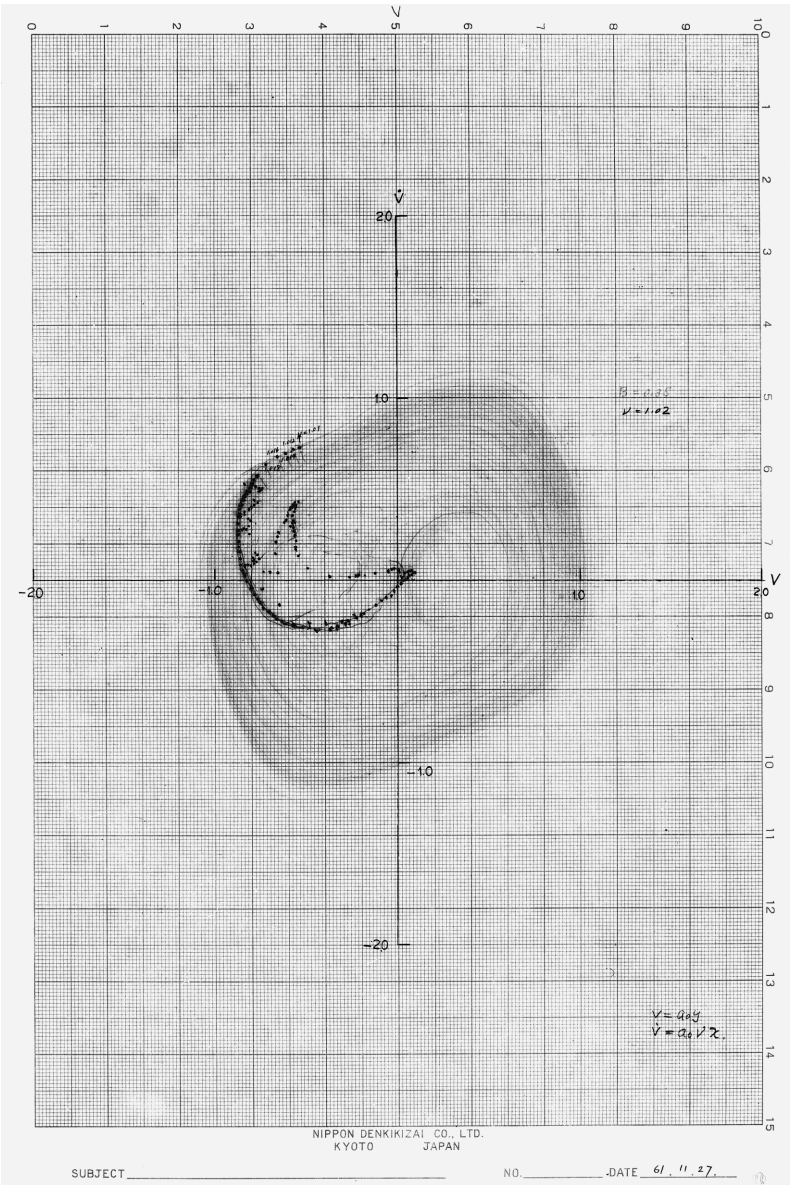

Fig. 1. Broken Egg Attractor first observed in physical system; the parameter values are $\mu = 0.2, \gamma = 8$, $B = 0.35$, and $\nu = 1.02$ – Brookhaven National Laboratory, Photography Division Negative No. 1-380-90

$$\frac{d^2u}{dt^2} - \mu(1 - \gamma u^2)\frac{du}{dt} + u^3 = B\cos \nu t, \quad 0 < \mu \ll 1 \tag{1}$$

with $\mu = 0.2, \gamma = 8$, and $B = 0.35$ obtained on 27 November 1961 is shown. A continuous trajectory is drawn lightly on the $(u, \dot{u})$ plane and points in the stroboscopic observation at phase zero are given by heavy dots: five dots near the top are fixed-points for a sequence of values at $\nu = 1.01, 1.012, 1.014, 1.016$ and 1.018, the remaining points are approaching and on the chaotic attractor at $\nu = 1.02$. Note that in the original data the variable v was used, but in this paper the dependent variable Roman letter v is replaced by u to avoid confusion with the parameter Greek letter nu.

That is, the bifurcation point is given by $B = 0.35$ and ν between 1.018 and 1.02. However, more accurate digital simulation gives ν between 0.99430 and 0.99431. Precision of analog computation depends on the combination of adders, integrators, and so on as well as temperature in the computer. The analog precision varies slightly every day. Very few mathematicians have direct experience with these practical effects on precision, however, it is proper that experimenters know these matters naturally. These experimental facts tell us in practical terms about the important mathematical concept of structural stability.

The main purpose of these computer experiments was to simulate the non-autonomous nonlinear differential equation describing synchronization phenomena Eq.1, and to examine the range of the frequency and amplitude of the driving signals which cause synchronization, as well as the amplitude and phase of its oscillation. The approximate computation was done by rewriting the non-autonomous equation into an autonomous equation applying the averaging principle. Approximation enters the process at this stage, with the result that chaos is suppressed. To be sure, in the early 60's, we didn't have even electronic calculators. Therefore, intense effort was required to get phase portraits of two-dimensional autonomous equations, for example via the isocline method, and other methods. The numerical calculation was done by using a Tiger Calucutator (Trade name of a mechanical calculating machine, a widely used and versalite machine in those days).

The aim of analog experiments was to verify the accuracy of the approximate autonomous equation obtained by averaging: how the steady states of the original system compare with an equilibrium point or limit cycle of the autonomous equation. Experience shows that if the approximation is good, a stable equilibrium point of the averaged, autonomous equation corresponds to synchronized periodic oscillation in the original non-autonomous system, and a stable limit cycle corresponds to asynchronous beat oscillation of the non-autonomous system.

Actually there are two kinds of asynchronous oscillations – quasi- or almost-periodic oscillation (represented approximately by a limit cycle in the averaged equation) and chaotic oscillation, corresponding to strange or chaotic attractors (which are not theoretically represented in the averaged equation): but the common sense of the day failed to recognize the chaotic oscillation. In those days and at present, only the equilibrium point and limit cycle were known to exist as steady states of a second order or two-dimensional autonomous system, so it was understandable for everyone to have possessed the preconceived notion that asynchronous condition meant quasi-periodicity. The Bendixon Theorem seemed to support this misconception.

On the day, the 27th of November 1961, when the author changed the parameter (frequency of the driving input), and condition shifted from frequency entrainment to asynchronization, the oscillation phenomena portrayed by his analog computer was chaotic indeed. It was nothing like the smooth oval closed curves, but was more like a broken egg with jagged edges. His first concern was that his analog computer had gone bad.

But he soon realized that was not the case. It did not take long for him to recognize the mystery of it all – the fact that in the asynchronous condition, the broken egg appeared more frequently than the smooth closed curves, and that the order of the dots which drew the broken egg was irregular, and at first seemed inexplicable. Figure 2 is an example of the waveform data made by the computer, which corresponds to Fig.1. Pulses or notches on the waveforms show stroboscopically the instants at phase zero of the driving signal which are introduced into the waveform, and momentarily perturb the output signal without giving effects to the main operational unit for Eq.1, i.e., by inserting buffer between output and main circuits. It reminds him of the long hours patiently sitting in front of the analog computer, and of his wonder at its accuracy. As he looks back, he feels that after those long exhausting vigils in front of the analog computer, staring at its output, chaos had become a totally natural, everyday phenomenon in his mind. There's nothing new about it – only people did not notice it.

(b) Detailed Outline for Broken Egg Phenomenon

This item introduces the experimental results which were obtained in 1961 by analog computer simulation as well as in 2006 by digital simulation. Figure 3 shows synchronization regions obtained by (*a*) by analog and (*b*) by digital computer simulations. The range of parameters was taken to cover problematic

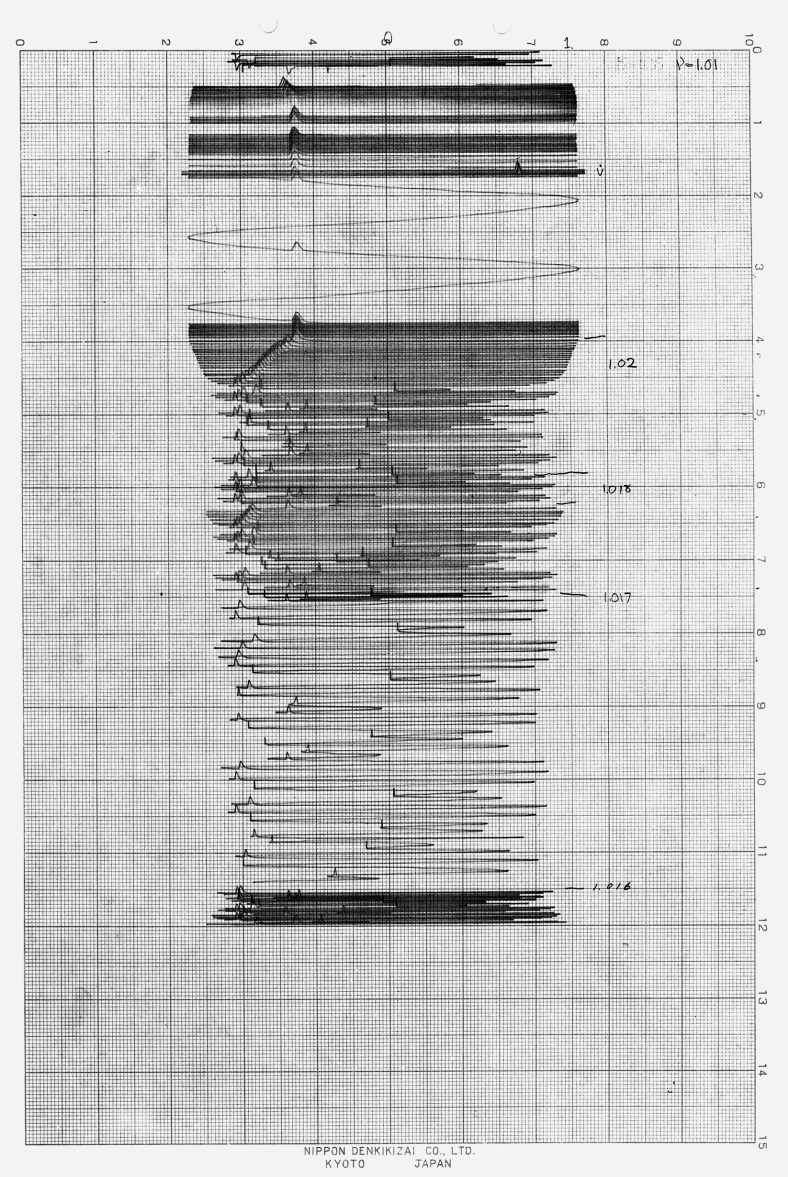

Fig. 2. Waveforms related to Broken Egg Attractor in Fig.1 – Brookhaven National Laboratory, Photography Division Negative No. 9-307-90

regions between entrainment and quenching. In the curvilinear delta areas AEC in both cases, two periodic synchronized oscillations occur depending on initial conditions, or detailed history of changing parameters. Readers can compare these with larger synchronization regions in Fig.4.2 of his Doctoral Thesis:
[http://repository.kulib.kyoto-u.ac.jp/dspace/bitstream/2433/68907/4/D_Ueda_Yoshisuke.pdf]
The curve segment EA shows Fold bifurcation, CE Hopf bifurcation. Entrainment and quenching are separated by the point E. However, in the shaded regions, asynchronous beat oscillations occur as well as entrained (resonant) oscillations. In other words, regions of asynchronized beat oscillations overlap with and/or enter into entrainment region. Due to the situation, bifurcation phenomena become complicated, and all the more interesting. Readers can look at some series of phase portraits of averaged autonomous systems in the author's Doctoral Thesis.

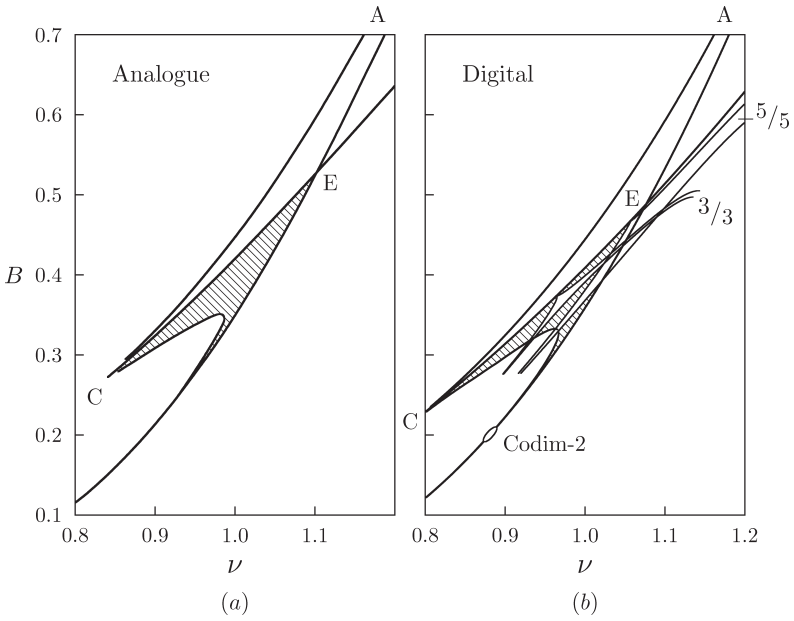

Fig. 3. Bifurcation sets around and between entrainment and quenching: (*a*) obtained by analog simulation in 1961 (*b*) by digital simulation in 2006

Figure 4 shows phase portraits of the system governed by Eq.1 with $\mu = 0.2, \gamma = 8, B = 0.35$, and $\nu = 0.99$, just inside of the entrainment region. Results are from digital simulations, taking only stroboscopically sampled points at phase zero, according to the transformation (or mapping) defined by using the solutions of Eq.1 to advance from one stroboscopic sampling to the next. In the figure, point S represents a completely stable fixed-point, which corresponds to entrained periodic oscillation. Point D represents a directly unstable fixed-point (saddle), and its α-branches and ω-branches are also drawn. The ω-branches of D form the basin boundary between S and the Broken Egg Attractor (BEgg). When the parameter is changed, i.e., ν is increased from 0.99 very gradually while $B = 0.35$ is kept unchanged, points S and D approach each other and coalesce at the value of ν between 0.99430 and 0.99431 forming a higher order fixed-point SD, which then disappears. The stroboscopic points take off from the (disappeared) SD point, move toward BEgg and then wander randomly on the BEgg forever.

(c) Reason Why the Author Attacked Eq.1

During the time the author was a Master's degree student, he had been engaged in analog computer experiments on the study of asynchronous (non-periodic) oscillations for a periodically forced self-oscillatory systems (Van der Pol Equation with External Forcing Term noted below as Eq.2) under the guidance of Prof. Shibayama.

$$\frac{d^2u}{dt^2} - \varepsilon(1-u^2)\frac{du}{dt} + u = B_0 + B\cos\nu t, \quad 0 < \varepsilon \ll 1 \tag{2}$$

In this system, phenomena (steady states) are summarized as follows:

- Without external driving signal, the system maintains intrinsic constant frequency and amplitude, so-called self-sustained oscillation which is represented by a limit cycle of the van der Pol Equation.
- Synchronization with the external force occurs depending on frequency and amplitude of the driving signal, that is, synchronization occurs when the control parameters (frequency and amplitude of the driving signal) are given in the synchronizing region.

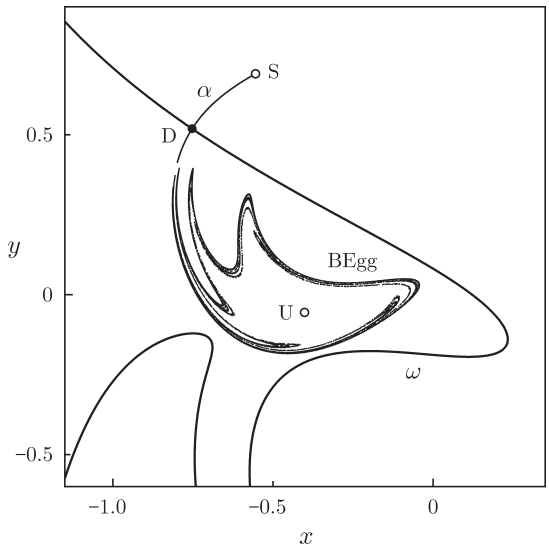

Fig. 4. Phase portrait of the Transformation defined by Eq.1 with $\mu = 0.2, \gamma = 8, B = 0.35$, and $\nu = 0.99$ (Note that x, y correspond to $u, du/dt$)

- When the control parameters are given outside of the synchronizing region, asynchronous beat (non-periodic) oscillation comes out.
- When parameter is varied across the boundary of synchronization, periodic oscillation changes to beat oscillation, or beat to periodic depending on the sense of change of the parameter. We referred to the phenomena as transition in those days; it is now called bifurcation, and the boundary of synchronization is the bifurcation set.
- Mechanism of synchronization in the system represented by Eq.2 is classified into the following two categories: Frequency Entrainment (Pull-in) and (Amplitude) Quenching. Frequency entrainment occurs for small values of the amplitude of the driving signal and small detuning (degree of difference between self-sustained and external driving frequencies), while quenching occurs for rather large amplitude and detuning.

  In current terminology, the former is known as a Fold or Node-Saddle bifurcation, and the latter a Hopf bifurcation. As the author was trained repeatedly by taking careful note of the output of analog computer, he could judge immediately what was the rough sketch of the phase portrait by glancing at the behavior of pulse or notch trains on the waveforms. In the system governed by Eq.2 asynchronous (beat) oscillations always traced out simple closed curves on the phase plane.
- The author was interested in “What’s going on between Entrainment and Quenching?”, however, the problematic regions in the system represented by Eq.2 were too narrow to attack via analog computer. This was the reason why Eq.1 was taken up. According to the author’s faint memory, Profs. Hayashi and/or Shibayama told him that Eq.1 was manufactured in order to have an example of a phase portrait in which both a stable equilibrium point and a limit cycle were found. However, at that time no additional information was given, e.g., its relation with the periodically forced negative-resistance oscillator, which will be stated below.

Mind-boggling vigils in front of computer had taught him to be able to notice something unusual – that is, Broken Egg became part of his awareness.

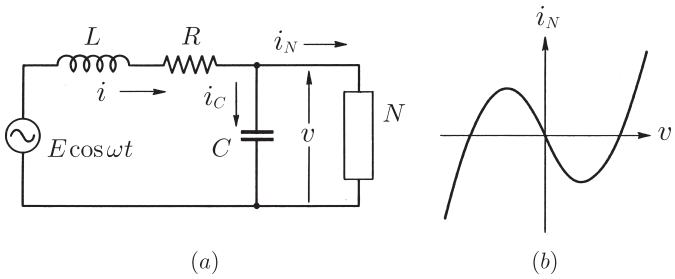

Fig. 5. (a) Periodically forced self-oscillatory circuit (b) Characteristics of negative-resistance element

3. The Road to Randomly Transitional Phenomenon

Professor Ralph H. Abraham (University of California at Santa Cruz), together with Dr. H. Bruce Stewart (Brookheaven National Laboratory), planned and published the present author's monograph entitled, "The Road to Chaos" [Aerial Press, Santa Cruz, CA 95061, 1992].

Due to the generosity of Prof. Ralph Abraham, a copy of the monograph was placed in the Repository of Kyoto University. It represents the present author's accomplishment before chaos becomes fashionable. [http://repository.kulib.kyoto-u.ac.jp/dspace/handle/2433/71101]

4. Follow-Up Experiment on the Broken Egg Phenomenon

In the preceding section 2, the chaotic BEgg phenomenon which appears in the periodically forced self-oscillatory system is introduced. The phenomenon was regarded as an actual physical phenomenon, e.g., observed in a custom analog computer using vacuum tubes. While it might be an actual physical phenomenon, the author had tried to observe BEgg phenomenon in a more natural electronic circuit. In this section, experimental results are given from another study conducted in accordance with the BEgg phenomenon [IECE, Technical Report, NLP72-13 (1972-12) in Japanese].

(a) Equation Derivation from Electronic Circuit

The circuit diagram illustrated in Fig.5 shows a periodically forced negative-resistance oscillator, in which self-sustained oscillation takes place due to the negative-resistance element when no external signal is injected. With the notation of the figure, the the equations for the circuit are written as

$$\left.\begin{aligned} L\frac{di}{dt} + Ri + v &= E\cos\omega t \\ i = i_C + i_N, \qquad i_C &= C\frac{dv}{dt} \end{aligned}\right\} \tag{3}$$

The negative-resistance element is manufactured with inverse parallel connected DC biased Esaki (or tunnel) diodes. We may assume the characteristic of this element to be the following cubic curve

$$i_N = -a_1 v + a_3 v^3, \qquad a_1 > 0, \quad a_3 > 0 \tag{4}$$

Then, after elimination of currents i, i_C and i_N in Eqs.3 and 4, the result in term of the voltage v is

$$LC\frac{dv^2}{dt^2} - (a_1 L - RC)\frac{dv}{dt} + 3a_3 L v^2 \frac{dv}{dt} + (1 - a_1 R)v + a_3 R v^3 = E\cos\omega t \tag{5}$$

By the inspection of Eq.5, the condition for maintaining self-sustained oscillation in the system governed by Eq.5 is given by the establishment of the inequality $(a_1 L - RC) > 0$. In the case of setting up circuit

conditions for the inequality to be satisfied, the Eq.5 is summarized as the following equation[2]

$$\frac{d^2x}{d\tau^2} - \mu(1-x^2)\frac{dx}{d\tau} + \alpha x + x^3 = B\cos\nu\tau \tag{6}$$

where

$$\left.\begin{aligned} x &= \sqrt{\frac{3a_3L}{a_1L-RC}}\,v, & \tau &= \sqrt{\frac{R(a_1L-RC)}{3L^2C}}\,t \\ \mu &= \sqrt{\frac{3}{RC}(a_1L-RC)}, & \alpha &= \frac{3L(1-a_1R)}{R(a_1L-RC)} \\ B &= \frac{3EL}{R}\sqrt{\frac{3a_3L}{(a_1L-RC)^3}}, & \nu &= \sqrt{\frac{3L^2C}{R(a_1L-RC)}}\,\omega \end{aligned}\right\} \tag{7}$$

The Eq.6 thus obtained is rewritten as a system of first order two-dimensional non-autonomous periodic equations

$$\left.\begin{aligned} \frac{dx}{d\tau} &= y \\ \frac{dy}{d\tau} &= \mu(1-x^2)y - \alpha x - x^3 + B\cos\nu\tau \end{aligned}\right\} \tag{8}$$

(b) Negative-Resistance Element

The negative-resistance element shown in figure 5 (*b*) was manufactured using Esaki (or tunnel) diodes. The problem "How to avoid parasitic oscillations due to stray capacitor and inductor?" presented an obstacle. By concentrating our sense and technology for overcoming difficulties, the element had been accomplished. However, for the author the most difficult problems were to persuade his students and colleagues of the significance, worth and aim of the experiment. Many hours were spent in the explanations. The students seemed to be satisfied after chaos became fashionable. It is a dear remembrance, as from yesterday. The details are abbreviated here, but the experiment succeeded. The negative-resistance element was manufactured in this way, and has current vs voltage characteristic as shown in figure 6. The dotted lines in the figure (*b*) are characteristics of DC biased E_0 (155 [mV]) Esaki-diodes which were inverse parallel connected. The currents i_{D_1} and i_{D_2} are shown in the figure (*a*). Their sum i_N is drawn with the heavy line. Approximation of the characteristic curve is given by the following equation

$$i_N = -0.028\,v + 1.364\,v^3 \tag{9}$$

where, units of i_N and v are [A] and [V], respectively. Note that the metal-film resistor ($R = 10$ [Ω]), and big condenser ($C = 20$ [mF]) for the impedance effect compensation were used.

(c) Experimental Results I

When the parameters in Eq.8 are specified by the following equations

$$\mu = 3.0, \quad \alpha = 0.0 \tag{10}$$

The following circuit constant values are selected [3].

[2] Eq.6 differs slightly from 1, that is γ is eliminated and α is introduced. Eq.1 is obtained from the electronic circuit in Fig.5(*a*) by re-arrangement.

[3] The following relations are derived from Eq.7

$$a_1R = \frac{9}{9 + \alpha\mu^2/(1+\mu^2/3)}, \quad a_1L = RC\left(1+\mu^2/3\right)$$

Inspecting these relations tells us that it becomes difficult to set small values for μ.

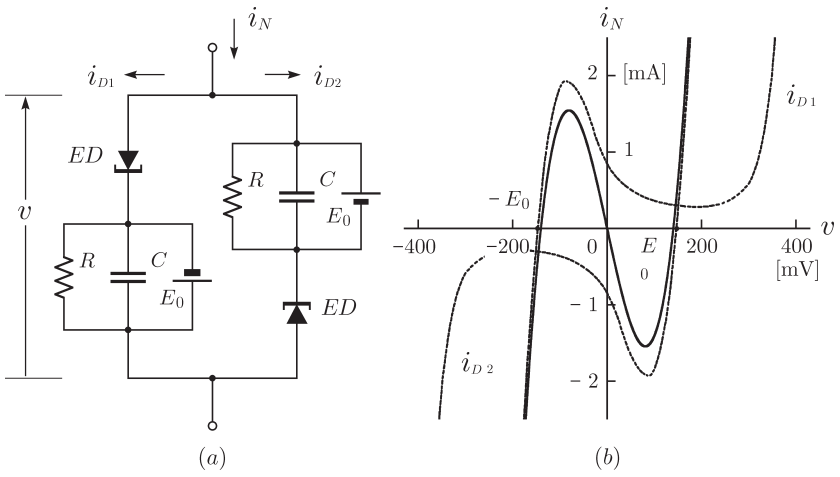

Fig. 6. Negative-resistance element: (*a*) Circuit composition (*b*) Voltage and current characteristic

$$R = 35.7\ [\Omega], \quad L = 47.1\ [\mathrm{mH}], \quad C = 9.20\ [\mu\mathrm{F}] \tag{11}$$

The frequency and amplitude (peak to peak value) of self-sustained oscillation of this case I are 171 [Hz] and 300 [mV]. The regions of the m/n harmonic oscillations observed in the circuit of the case I, and more detailed data about the experiment are given in the following URL. Note that m/n harmonic implies the oscillation having n-times the period of the external signal as its fundamental component, and the m-th order higher harmonic is predominant. [http://repository.kulib.kyoto-u.ac.jp/dspace/bitstream/2433/24278/1/111-126.pdf] And yet Figure 7 shows various types of waveforms of asynchronized (non-periodic) beat oscillations.

(d) Experimental Results II

When parameters in Eq.8 are setup by the following equations

$$\mu = 3.0, \quad \alpha = -1.8 \tag{12}$$

The following circuit constant values are selected.

$$R = 64.9\ [\Omega], \quad L = 118\ [\mathrm{mH}], \quad C = 12.7\ [\mu\mathrm{F}] \tag{13}$$

In this case II, no self-sustained oscillation is maintained in the circuit. When no signal is injected to the circuit of the case II, system sleeps in silence on a equilibrium point, which will be shown in the following item. In spite of having no self-sustained oscillation, qualitatively similar regions to the case I appear in the circuit II. Figure 8 shows various asynchronous waveforms for the control parameter, given outside the synchronized m/n regions.

(e) Remarks on the Experimental Results

Though we could not observe the same BEgg oscillation in our circuit, the Broken Egg Phenomenon seems a rather universal one which occurs in periodically forced self-oscillatory second-order systems with hard type nonlinear restoring term, when the frequency of the external signal is higher than self-oscillatory frequency (see the folllowing item).

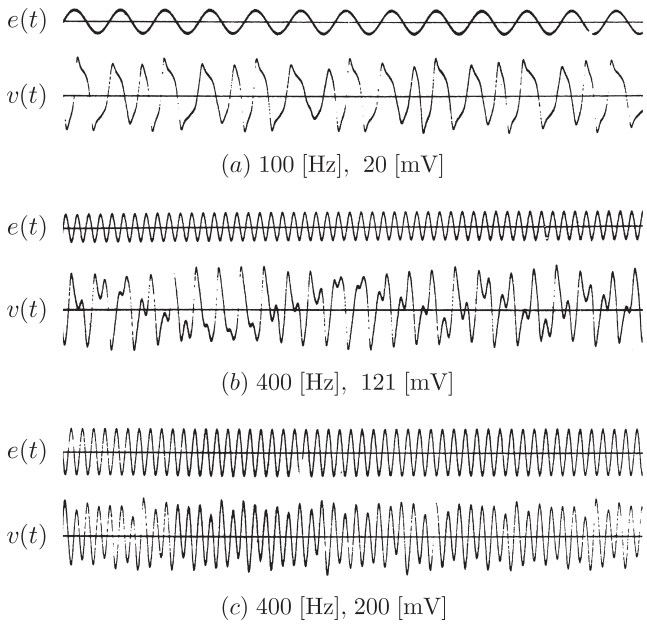

Fig. 7. Various waveforms of asynchronous beat oscillations in the circuit I

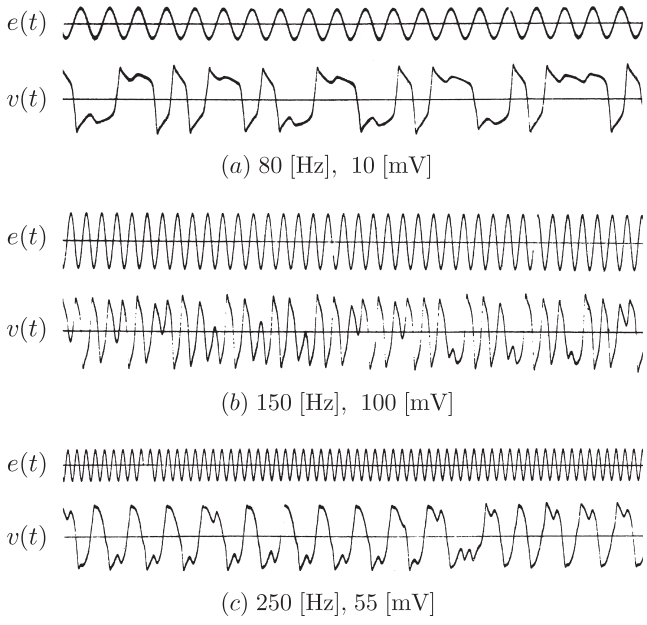

Fig. 8. Various waveforms of asynchronous best oscillations in the circuit II

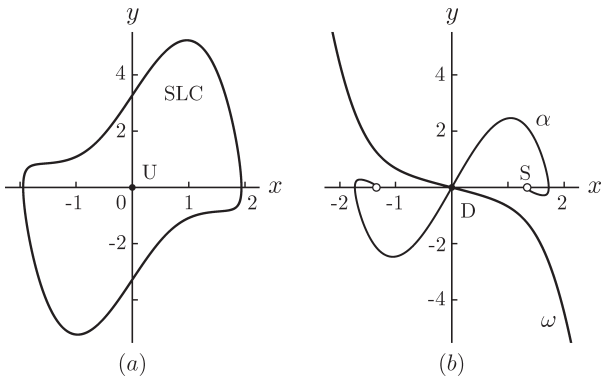

Fig. 9. Phase portraits without forcing signal for the cases I and II

Regarding the value of the parameter $\mu = 3.0$, in those days it seemed about the smallest value that could be realized in a circuit of this type with precision components [4]. The value of $\mu = 3.0$ was deemed to be rather large for simulation study. It seems to supress varieties of phenomena, as well as to bring abrupt changes in variables, i.e., the relaxation oscillation tendency has been seen, and in the numerical experiments strongly unbalanced values of characteristic multipliers of fixed- or periodic-points would cause difficulties.

Figure 9 shows phase portraits for the circuits of the case I and II when the external signal is removed. A limit cycle representing self-sustained oscilllation exists in Fig.9 (*a*), while in Fig.9 (*b*) there is no limit cycle, but two equilibrium points take place. This figure implies that a limit cycle ceases to exist at some bifurcation point when α is decreased from zero.

Though in the case II there is no limit cycle, qualitative similarity is seen when an external forcing signal is applied. Apart from synchronized periodic oscillations, there is a decisive difference between asynchronous regions of the case I and II. As there is no completely unstable fixed-point (source) in the case II, every asynchronous oscillation is chaotic represented by chaotic attractor. However, in the case I, among asynchronous beat oscillations there will be quasi- or almost-periodic oscillation represented by invariant closed curve as well as chaotic oscillations. Inspectig the waveforms, Fig.7 (*a*) and all in Fig.8 are chaotic oscillations, while that of Fig.7 (*b*) and (*c*) seem to be almost-periodic oscillations. Author's guess about these must be suspended. However, waveform of Fig.7 (*c*) may be almost-periodic oscillation just before quenching, represented by a small invariant closed curve.

Through this experimental study, the author realized the following difficulties from the bottom of his heart.

- To let others make up their own minds, i.e., to make fully understood the author's intention without appealing to authority.
- There is an unavoidable difference between actual and theoretical worlds on one level or another.

5. Phenomena Occurring in Periodically Forced Self-Oscillatory Systems (PFSOS)s

In order to make clear the whole range of phenomena which can occur in PFSOSs, some preliminary considerations are given, in the system governed by the following second-order ordinary differential equation (ODE)

[4] At present the circumstance is supposed to be unchanged, but almost all electronic circuits are replaced with LSI circuits or systems.

$$\frac{d^2x}{dt^2} + \varepsilon f\left(x, \frac{dx}{dt}\right)\frac{dx}{dt} + g(x) = F\cos\nu t, \quad 0 < \varepsilon \ll 1 \tag{14}$$

where functions $f(x, y)$ and $g(x)$ are assumed as polynomials or elementary functions with respect to x and y $(= dx/dt)$.

The role of restoring, dissipative (damping) and forcing term is summarized below.

- Restoring Term: When $\varepsilon = 0$ and $F = 0$, the Eq.14 is rewritten into the following two-dimensional autonomous equation

$$\left.\begin{aligned} \frac{dx}{dt} &= y \\ \frac{dy}{dt} &= -g(x) \end{aligned}\right\} \tag{15}$$

  The above conservative system is integrable, and a family of closed curves is drawn on the (x, y) phase plane. Every closed curve represents a periodic solution of Eq.15, however, it is unstable in the sense of Lyapunov unless g is linear. The function $g(x)$ enriches the varieties of oscillatory phenomena, as will be shown below.

- Dissipative Term: When $0 < \varepsilon \ll 1$ and $F = 0$, the Eq.14 is rewritten into

$$\left.\begin{aligned} \frac{dx}{dt} &= y \\ \frac{dy}{dt} &= -\varepsilon f(x, y)y - g(x) \end{aligned}\right\} \tag{16}$$

  In general, the existense of a damping term f makes the system, Eq.16, non-integrable. The term brings dissipative effects into the system, and it selects limit cycle(s) among the family of closed curves. Of course, appearance of limit cycle(s) depends on the specification of the function f. Stable limit cycle(s), if it exists, represent self-sustained oscillation(s), and unstable limit cycle(s) give(s) basin boundary(ies).

- External Forcing Term: When $0 < \varepsilon \ll 1$ and $F \neq 0$, the Eq.14 is rewritten into

$$\left.\begin{aligned} \frac{dx}{dt} &= y \\ \frac{dy}{dt} &= -\varepsilon f(x, y)y - g(x) + F\cos\nu t \end{aligned}\right\} \tag{17}$$

  The system represented by the above Eq.17 is a non-autonomous periodic system with period $2\pi/\nu$, which defines the transformation T or mapping M of the (x, y) plane into itself, i.e., a one-to-one, continuous, and orientation-preserving transformation or mapping. Thus a discrete dynamical system is defined using solutions of the Eq.17. The author likes to call it stroboscopic observation at phase zero of phenonena. Attention should be paid to the existence interval of solutions of the Eq.17 on the t-axis, that is, solutions may diverge to infinity at finite backward time due to the specification of $f(x, y)$. Therefore, the concept of class D becomes important, i.e., dissipative systems for large displacement introduced by N. Levinson.

  In the system represented by Eq.17, global appearance of the behavior is represented by phase portraits under the transformation T. Steady states are represented by attractors in the phase portraits. Every attractor resides in its basin. Generally, there are some attractors in the phase portraits. In otherwords, phase portraits are divided into several basins by its (basin) boundaries. Among attractors, regular (predictable) phenomena are given by minimal sets composed of fixed-points, periodic-points, and/or invariant closed curves. However, irregular (unpredictable) phenomena are given by chaotic attractors composed of homoclinic tangle of outsets (α-branches) from saddle type fixed- or periodic-points. In

the chaotic attractor, the actual (observable in physical system or in computer simulation) movement of representative point wanders randomly among the infinitely many (dense) unstable periodic solutions due to unavoidable small uncertain quantities, such as noise or parameter (or characteristics of elements) fluctuations in systems. Thus, irregular (stochastic) behavior occurs in actual physical (deterministic) systems based on the global (deterministic) structure of solutions of ODEs. It should be noted that minute systems (parameters) fluctuation isn't avoided. Based on the above points of view, the author called the phenomenon as "randomly transitional phenomenon" before the term "Chaos" was coined by T. Y. Li and J. Yorke, or R. May. Chaotic or strange attractors were composed of closure of outsets (α-branches) in which infinitely many saddle type periodic-points were contained. Let us call the shortest period of saddle type (fixed- or) periodic-point in the attractor as principal period of chaotic attractor[5]. The principal period is also useful to characterize attractors via index theory [Stewart, H.B., Application of Fixed Point Theory to Chaotic Attractors of Forced Oscillators, Japan Journal of Industrial and Applied Mathematics, **8** (1991), 487-504].

Let us discuss the maginitude of the small parameter ε. In actual physical or engineering systems, determination of so-called damping or dissipative parameter value is a difficult problem, as is system identifications, especially for large scale ones. In practice, the mathematical concept of small parameter is sometimes invoked in a somewhat arbitrary or artificial manner[6]. However, the author recognizes and appreciates the effectiveness of the concept of small parameter for the analysis of nonlinear problems.

Putting aside generalizations, the numerical values used in the following examples are settled based on judgement from the author's experience. In the following examples, the parameter ε or μ seems to be given at moderate or proper values for theoretical models of nonlinear phenomena. When the parameter value is increased, transients are shorter in duration, varieties of the phenomena decrease, the tendency of relaxation oscillations increases, and difficulty of numerical experiment increases. When the parameter value is decreased, transient duration becomes longer, varieties of phenomena increases, and chaotic attractor, if it exists, becomes bigger and thicker. Finally, changing the parameter to zero, a chaotic attractor sometimes tends to a chaotic sea in the generating conservative system

$$\left.\begin{aligned} \frac{dx}{dt} &= y \\ \frac{dy}{dt} &= -g(x) + F\cos\nu t \end{aligned}\right\} \tag{18}$$

via periodic-points that appear in windows of parameter values, as observed in the iterated maps. Attention should be paid to the change of the chaotic sea, transitions that occur as the chaotic sea disappears, and periodic-points replace it for sufficiently small non-zero values of the parameter, because of the existence of islands in the chaotic sea. The islands are replaced by completely stable and/or unstable (fixed- or) periodic-points (sinks and/or sources) in the dissipative systems, when small values of the parameter are given. It is needless to say that numerical experiments for the conservative system Eq.18 will require appropriate care.

With this general preparation we introduce some concrete examples.

(a) Preparation I

Modification of the damping term in Van der Pol's equation brought no remarkable qualitative and quantitative changes of its limit cycle. That is, numerical experiment of the following ODE by varing c_2 (or c_4) between 0 and 1 keeping the relation $c_2 + c_4 = 1$, guaranteed the above statements for a rather wide range of μ [IEICE, Technical Report, NLP2004-24 (2004-07) in Japanese].

$$\left.\begin{aligned} \frac{dx}{dt} &= y \\ \frac{dy}{dt} &= -\mu(1 - c_2x^2 - c_4x^4)y - x \end{aligned}\right\} \tag{19}$$

[5]The principal period of the Broken Egg attractor is period 3 or $6\pi/\nu$.

[6]Once a parameter value is fixed, then it becomes a constant and is no longer a parameter, however small its value may be.

(b) Preparation II

Synchronization phenomena in the system having Van der Pol type damping term and Duffing type restoring type, i.e.,

$$\frac{d^2x}{dt^2} - \mu(1-\gamma x^2)\frac{dx}{dt} + x^3 = F\cos\nu t, \quad 0 < \mu \ll 1 \tag{20}$$

and in the system having Rayleigh type damping term and Duffing type restoring type, i.e.,

$$\frac{d^2x}{dt^2} - \mu\left[1-\gamma^2\left(\frac{dx}{dt}\right)^2\right]\frac{dx}{dt} + x^3 = F\cos\nu t, \quad 0 < \mu \ll 1 \tag{21}$$

were discussed in the author's doctoral thesis. The frequency response curves of fundamental harmonics, i.e., $\cos\nu t$ and $\sin\nu t$ components, and their stability limits were quite similar, especially when the frequency ν took a larger value than that of self-oscillatory frequency ω_0. The remarkable difference between Eqs.20 and 21 developed in the stability limit representing Hopf bifurcation or quenching boundaries when the frequency ν took smaller value than that of self-oscillatory frequency ω_0. This was the reason why the author attacked Eq.21.

(c) Preparation III

Averaging principle for the analysis of second-order non-autonomous Eq.14 was proved to be greatly effective method to derive two-dimensional autonomous system for small parameter ε, which represents the global aspect of fundamental component.

The author noticed that the following Eq.22

$$\left.\begin{aligned}\frac{dx}{dt} &= y - \mu f(x,y)x \\ \frac{dy}{dt} &= -\mu f(x,y)y - g(x) + F\cos\nu t\end{aligned}\right\} \tag{22}$$

is not equivalent to Eq.14, but the same autonomous system comes out via averaging principle from both Eqs.14 and 22 for $\varepsilon = 2\mu$. This fact implies that, as far as the predominant fundamental components of the oscillatory phenomema are concerned, Eqs.14 and 22 produce the same outcomes; the systems 14 and 22 behave in ways that have much in common. Moreover, in the system 22 the effect of dissipation is applied to both the variables x and y, i.e., variation is decreased by distributing the dissipation. The validity of numerical simulation increases, although for the variable y, the interpretation as the velocity of x is lost.

(d) Proposal for PFSOSs

Based on the above preparations inclusively, the following systems are proposed as prescriptive examples having hard type and soft type restoring terms of the PFSOSs.

- PFSOS with Hard Type Restoring Term

$$\left.\begin{aligned}\frac{dx}{dt} &= \mu(a^4 - x^4 - 2y^2)x + y \\ \frac{dy}{dt} &= -x^3 + \mu(a^4 - x^4 - 2y^2)y + F\cos\nu t\end{aligned}\right\} \tag{23}$$

where μ is a small parameter, a determines the amplitude of self-sustained oscillation. Cotrol parameters F and ν are the amplitude and (angular) frequency of the external forcing signal, respectively.

- PFSOS with Soft Type Restoring Term:

$$\left.\begin{aligned} \frac{dx}{dt} &= \mu(a + 2\cos x - y^2)x + y \\ \frac{dy}{dt} &= -\sin x + \mu(a + 2\cos x - y^2)y + F\cos \nu t \end{aligned}\right\} \tag{24}$$

where μ is a small parameter, a determines the amplitude of self-sustained oscillation. Cotrol parameters F and ν are the amplitude and (angular) frequency of the external forcing signal, respectively. Attention should be paid to the value of a, that is, when $a > 2$ the self-sustained oscillation becomes self-sustained rotation [7].

In such case, for numerical experimental study, the Eq.24 should be returned to the following second-order equation

$$\left.\begin{aligned} \frac{dx}{dt} &= y \\ \frac{dy}{dt} &= -\sin x + \varepsilon(a + 2\cos x - y^2)y + F\cos \nu t \end{aligned}\right\} \tag{25}$$

because of the diverging variable x. In the system governed by Eq.25, the dynamical range of x can be limited in the interval $(-\pi, \pi]$ without loss of generality. Then the phase portrait is drawn on the cylindrical surface.

It should be noted that the systems Eqs.23, 24 and 25 are all symmetric systems. That is, their invariance holds under the substitution $-x \to x$, $-y \to y$ and $t \to t + \pi/\nu$. The symmetry of the equations implies that a periodic trajectory is either symmetric to itself with respect the origin of the (x, y) plane or it coexists with another periodic trajectory symmetric to it with respect to the origin.

Readers can get summarized knowledge about Nonlinear Dynamics in the following URL:
[http://repository.kulib.kyoto-u.ac.jp/dspace/bitstream/2433/71101/3/Ueda_06.pdf]

(e) PFSOS with Hard Type Restoring Term

When the external signal is removed, the limit cycle representing self-sustained oscillation is given by the following equation for $a = 1.0$

$$x^4 + 2y^2 = 1 \tag{26}$$

and applying the variable transformation $x = \cos\theta$ its period T is given by

$$T = 4\sqrt{2}\int_0^1 \frac{dx}{\sqrt{1 - x^4}} = 4\sqrt{2}\int_0^{\pi/2} \frac{d\theta}{\sqrt{1 + \cos^2\theta}} \simeq 7.4163 \tag{27}$$

From the above, the (angular) frequency ω_0 of the self-sustained oscillation is given by the following relation

$$\omega_0 = \frac{2\pi}{T} \simeq 0.8472 \tag{28}$$

We are now ready to present the results of simulations of the prescriptive system with hard type restoring term Eq.23. The detailed bifurcation diagrams are shown in map of the (ν, F) parameter planes with fixed $\mu = 0.1$ and $a = 1.0$ in the following text book.
[Ueda. Y,"Theory of Chaotic Phenomena", 2008, CORONA PUBLISHING CO., LTD. Tokyo Japan.
ISBN 978-4-339-02611-5 http://www.coronasha.co.jp]

[7] It is well known that in two-dimensional autonomous systems limit cycle represents self-sustained oscillation. This interpretation is natural and acceptable for limit cycle represented by a simple closed curve on a plane. However, for the limit cycle of the so-called second kind represented by headband of cylindrical phase surface, application of the term self-sustained rotation should be careful in relation with the specifications of functions $f(x, y)$ as well as $g(x)$.

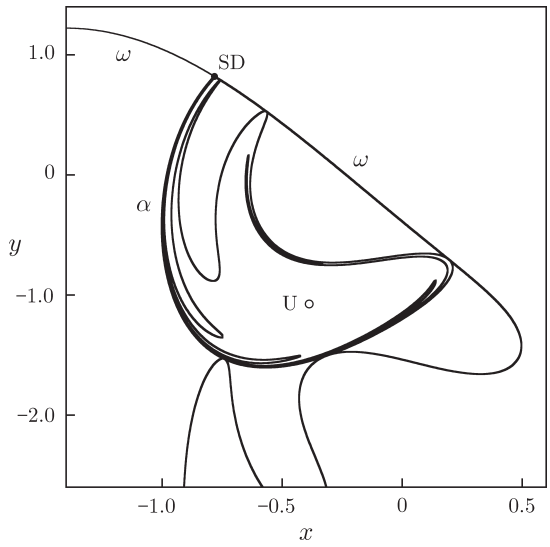

Fig. 10. Phase portrait with codimension-2 point corresponding to Fig.3 (b) in Eq.23 with $\mu = 0.1, a = 1.0$

The phase portrait corresponding to Codim-2 higher order bifurcation point in Fig.3 (b) is drawn in Fig.10. This portrait constitutes a core element of an old mystery which the author has long pondered, originating from between Entrainment and Quenching.

The steady states (attractors) outside the synchronization regions are given in Fig.11. This figure shows that the BEgg shaped chaotic attractors seem to be rather general phenomena observed in PFSOSs with hard type restoring terms for the (angular) frequency $\nu > \omega_0$.

Some examples of chaotic attractors are shown in Fig.12 which are observed for the (angular) frequency $\nu < \omega_0$. From the above, it seems difficult to draw global bifurcation sets (curves) or so-called Crisis sets on the (ν, F) plane as well as to classify chaotic attractors.

(f) PFSOS with Soft Type Restoring Term

When the external signal is removed, the limit cycle representing self-sustained oscillation is given by the following equation for $a = 1.0$

$$1 + 2\cos x = y^2 \tag{29}$$

and its period T by

$$T = 4\int_0^{2\pi/3} \frac{dx}{\sqrt{1 + 2\cos x}} \simeq 8.6261 \tag{30}$$

From the above, the (angular) frequency ω_0 of the self-sustained oscillation is given by the following relation

$$\omega_0 = \frac{2\pi}{T} \simeq 0.7284 \tag{31}$$

The results of simulations of the prescriptive system with soft type restoring term Eq.24 are shown in map of the (ν, F) parameter planes with fixed $\mu = 0.1$ and $a = 1.0$.

Figure 13 shows the bifurcation diagram for Eq.24 for the (angular) frequency $\nu > \omega_0$. In this map of the (ν, F) plane, the bifurcation sets (curves) of fundamental harmonics are drawn with somewhat heavier lines, and categories of bifurcation are also attached as Fold, NeiSac and Hopf. The curve segment indicated NeiSac is a Neimark and Sacker bifurcation set, known as inverse Hopf bifurcation, i.e., an unstable fixed-point changes to a stable fixed-point, casting off an unstable invariant closed curve.

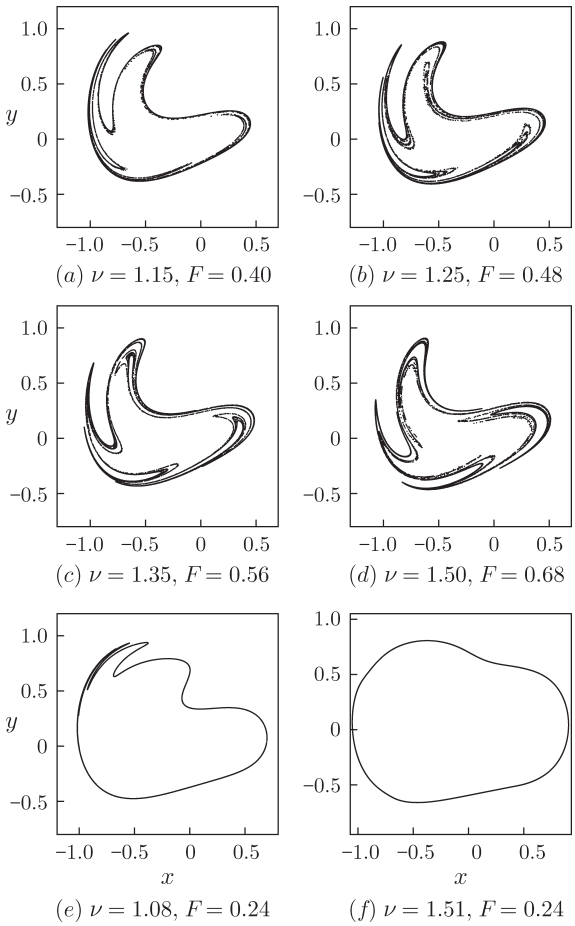

(a) $\nu = 1.15$, $F = 0.40$ (b) $\nu = 1.25$, $F = 0.48$

(c) $\nu = 1.35$, $F = 0.56$ (d) $\nu = 1.50$, $F = 0.68$

(e) $\nu = 1.08$, $F = 0.24$ (f) $\nu = 1.51$, $F = 0.24$

Fig. 11. Attractors representing asynchronous oscillations in Eq.23

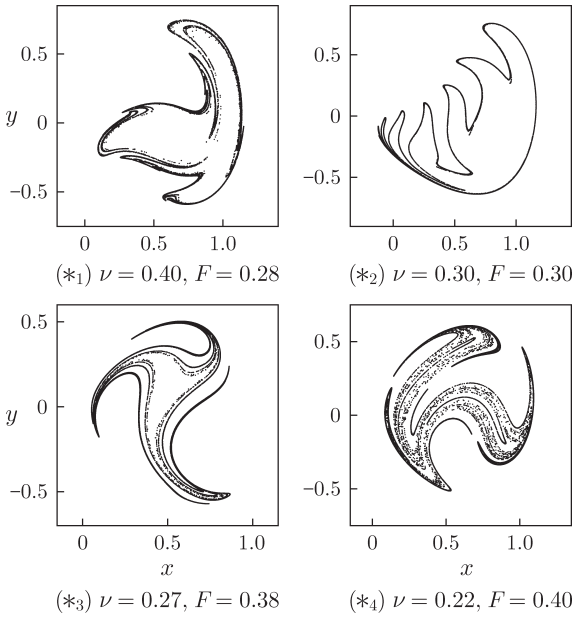

($*_1$) $\nu = 0.40$, $F = 0.28$ ($*_2$) $\nu = 0.30$, $F = 0.30$

($*_3$) $\nu = 0.27$, $F = 0.38$ ($*_4$) $\nu = 0.22$, $F = 0.40$

Fig. 12. Chaotic attractors of Eq.23 with $\mu = 0.1, a = 1.04$; Group (*)

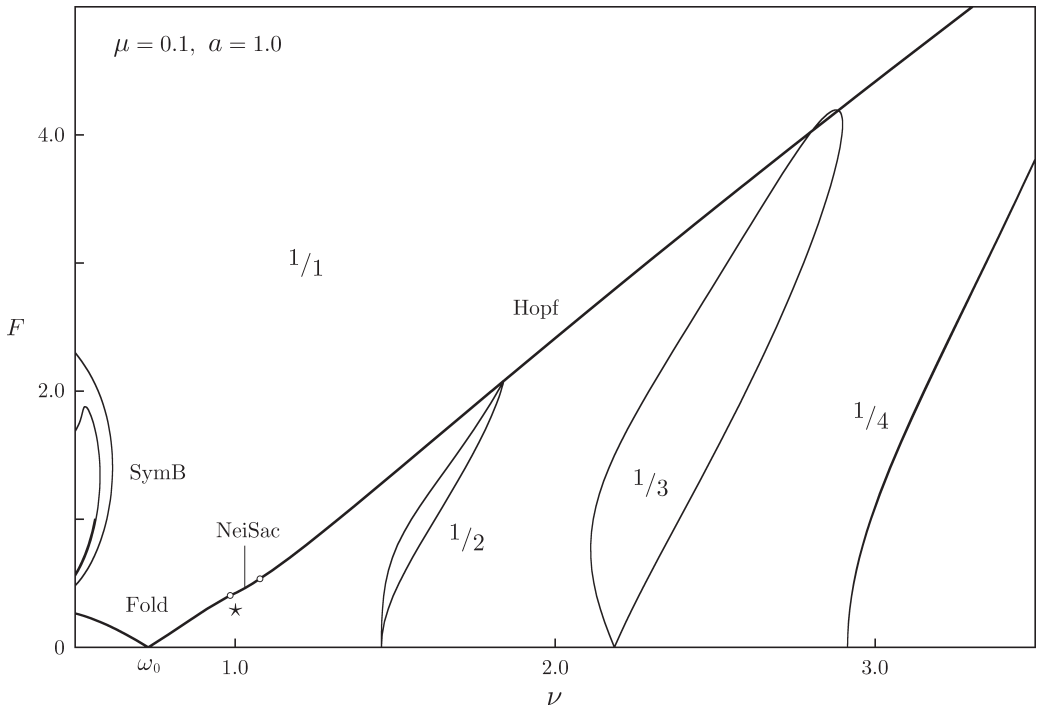

Fig. 13. Bifurcation diagram for Eq.24 with $\mu = 0.1, a = 1.0$ for $\nu > \omega_0$

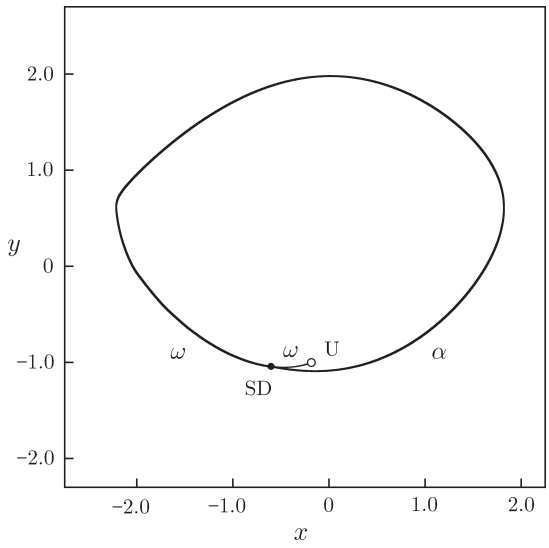

Fig. 14. Phase portrait with codimension-2 at Star Mark in Fig.13

Attention should be paid to the $1/1$ region (both the numerator and the denominator are odd), that is, a periodic trajectory is symmetric to itself with respect to the origin; thus after the symmetry breaking bifurcation indicated by SymB, period-doubling starts. Indeed, there exist two periodic trajectories symmetric with each other while at first the period is unchanged at $2\pi/\nu$, and continuing a parameter motion in this

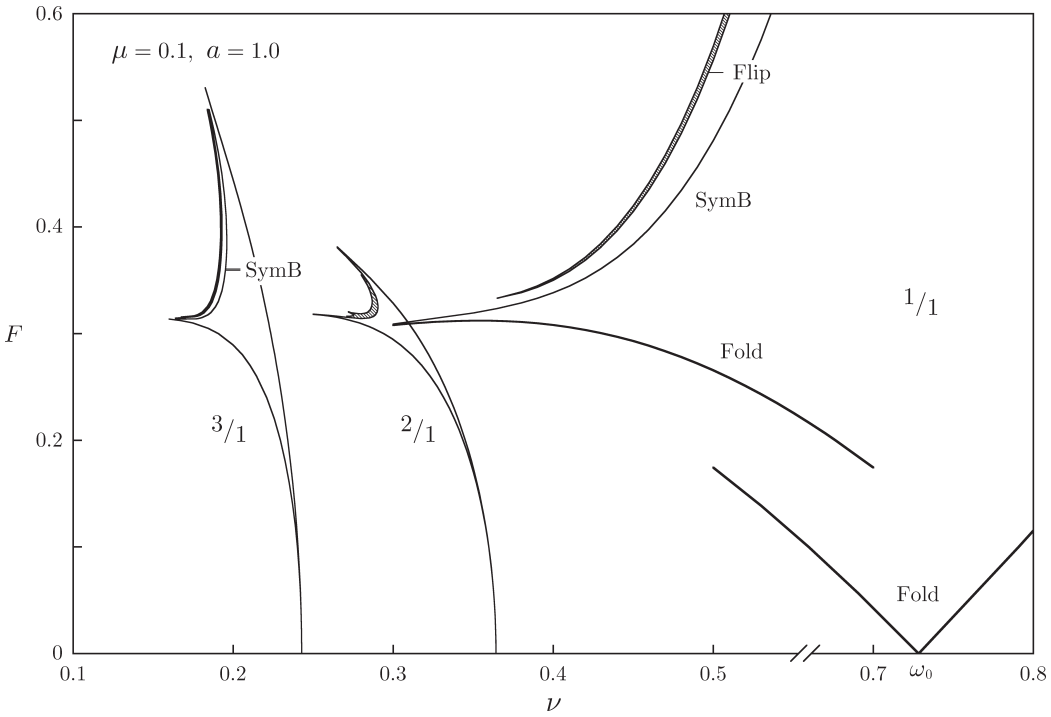

Fig. 15. Bifurcation diagram for Eq.24 with $\mu = 0.1, a = 1.0$ for $\nu < \omega_0$

direction leads, by a period-doubling cascade, to a $2/2$ region...

All bifurcation sets except indicated by small circles are codimension-one local bifurcations (the top of $1/2$ region seemed to be codimension-two). The small circle indicated by star mark on the bottom of the NeiSac bifurcation set is a codimension-two bifurcation where a global bifurcation curve terminates. That is, there exists thin regions along to the left side of the NeiSac arc in which a stable fixed-point and stable invariant closed curve coexist and their basins are separated by the unstable closed invariant curve just cast off. On the left edge of the region stable and unstable invariant closed curves coalesce and then disappear. This region is too thin to draw in the Fig.13, i.e., to draw this global bifurcation curve seems difficult. Figure 14 shows phase portrait at the codimension-two point attached with star mark in Fig.13. This portrait constitutes a core element of questions originating from between Entrainment and Quenching in the system represented by Eq.24. On the top of the NeiSac segment, only a higher order fixed-point exists on the (x, y) phase plane.

When the parameter is changed across the NeiSac segment, phenomenon similar to the series of portraits shown in Fig.5.5 of the author's doctoral thesis may be observed, perhaps.

The $2/1$ and the $3/1$ regions in Fig.15 have a roughly similar shape, respectively. There are tongue-shaped shaded crescent regions. The shaded crescent within the $2/1$ harmonic region is a $4/2$ harmonic region, and a parameter change from the $2/1$ region into the shaded crescent cause a period-doubling bifurcation. The thin tongue-shaped shaded crescent within the $3/1$ region appears after SymB bifurcation.

Attention should be paid to both the $2/1$ and the $3/1$ regions, practically undetectable tongues exist near the bottom of the period-doubling bifurcation sets, and also the structure of extremities seems not simple like cusp. Minute structures may be found. The same situation occurs at the left edge of $2/2$ shaded region left or above the SymB bifurcation within $1/1$ region.

In the left upper part of the (ν, F) plane in Fig.15, there are many miscellaneous complex phenomena, however, these are unexplored.

6. Conclusion

The prescriptive systems are proposed in order to survey the phenomena which occur in periodically forced self-oscillatory systems. That is, the systems governed by the Eqs.23, 24 and 25 are given.

Among various steady states, regular (predictable) phenomena and their bifurcation sets are presented, covering all such phenomena that are readily observed, perhaps excepting some phenomena of so-called second kind which occur in the system represented by the Eq.25.

Various chaotic attractors are also collected, and it is shown that global bifurcations and classification of chaotic attractors are often related, but it seems to be extremely difficult to describe them completely.

Acknowledgments

The author requested Dr. Hugh Bruce Stewart to review and to check the contents of this article with historical accuracy, and he kindly agreed. The author would like to express his sincere thanks to Dr. H. B. Stewart.

Details of the BEgg attractor

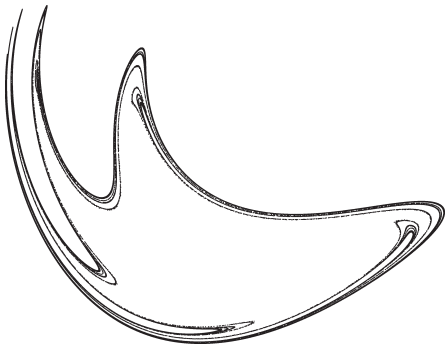

$$\left.\begin{aligned}\frac{dx}{dt} &= y \\ \frac{dy}{dt} &= 0.2(1-8x^2)y - x^3 + 0.35\cos t\end{aligned}\right\}$$